Construction of tight-binding-like potentials on the basis of density-functional theory: Application to carbon

D. Porezag,* Th. Frauenheim, and Th. Köhler
Technische Universität, Institut für Physik, Theoretische Physik III, D-09009 Chemnitz, Germany

G. Seifert and R. Kaschner
Technische Universität Dresden, Institut für Theoretische Physik, Mommsenstrasse 13, D-01062 Dresden, Germany
(Received 2 November 1994)

We present a density-functional-based scheme for determining the necessary parameters of common nonorthogonal tight-binding (TB) models within the framework of the linear-combination-of-atomic-orbitals formalism using the local-density approximation (LDA). By only considering two-center integrals the Hamiltonian and overlap matrix elements are calculated out of suitable input densities and potentials rather than fitted to experimental data. We can derive analytical functions for the C-C, C-H, and H-H Hamiltonian and overlap matrix elements. The usual short-range repulsive potential appearing in most TB models is fitted to self-consistent calculations performed within the LDA. The calculation of forces is easy and allows an application of the method to molecular-dynamics simulations. Despite its extreme simplicity, the method is transferable to complex carbon and hydrocarbon systems. The determination of equilibrium geometries, total energies, and vibrational modes of carbon clusters, hydrocarbon molecules, and solid-state modifications of carbon yield results showing an overall good agreement with more sophisticated methods.

I. INTRODUCTION

Currently, various theoretical concepts are applied to perform total-energy calculations on extended structures. Classical concepts, typically based on the construction of *empirical* potentials,[1,2] using data provided by experiments or *ab initio* methods, are very fast and successful if the physical properties of the investigated structures are well understood. However, such methods often fail to describe geometries not included in the data basis used for their construction.

On the other hand, there are accurate *ab initio* calculations based on density-functional (DF) (Refs. 3–6) or Hartree-Fock (HF) (Ref. 7) theory, which represent without any doubt a very reliable benchmark for all other methods. Although there has been much success in applying these methods to ever larger systems, they are still too slow for the investigation of many interesting problems.

Due to the limitations in the transferability of empirical potentials and the use of time consuming *ab initio* methods, *semiempirical* techniques have been developed to simulate extended systems with reasonable computational costs. In addition to numerous traditional quantum chemical methods, tight-binding schemes have been very successful.[8–10] In many cases, the results of these two-center-oriented schemes deviate only slightly from those of more sophisticated methods. However, the usual way of fitting the matrix elements necessary to calculate the band structure energy to an arbitrary set of input data is rather complicated and not very straight forward.

Our method tries to avoid the difficulties arising from an empirical parametrization by calculating the elements of Hamiltonian and overlap matrices out of a local orbital basis with the help of density-functional theory–local-density approximation (DFT-LDA) and some integral approximations. For that reason, it can be seen as an approximate linear-combination-of-atomic-orbitals (LCAO) -DFT scheme yielding exactly the same energy expression as common nonorthogonal tight-binding (TB) schemes. The only, but important, difference is that there is a well-defined procedure on how to determine the desired matrix elements. For that reason, we will refer to our method as a nonorthogonal DF-based TB scheme. As in usual TB ansatzes, only two-center Hamiltonian matrix elements are treated, and the short-range repulsive part of the total potential needs to be fitted with respect to self-consistent-field (SCF)-LDA data. Despite the extreme simplicity of this approach compared to SCF (Refs. 3 and 4) and *ab initio* calculations using the *Harris functional*,[6] the method has proven to be transferable to complex carbon and hydrocarbon systems. In this way, we support discussions in the literature[6,10,11] that nonorthogonality is a key to transferability.

This paper is organized as follows. In Sec. II, we briefly outline the method and describe the construction of Hamiltonian and overlap matrix elements and the short-range repulsive potential. Since we are mainly interested in investigating a variety of carbon systems incorporating hydrogen, we applied our method to these systems as described in Sec. III and present analytical functions for all Hamiltonian and overlap integrals versus interatomic separation for C-C, C-H, and H-H interactions. In Sec. IV, we summarize the results of the calculations performed on small clusters, fullerenes, hydrocarbons and solid state modifications to test the strengths and limits of the DF-TB model. Our findings are compared to experimental data and *ab initio* calculations.

II. METHOD

Our method, based on the work of Seifert, Eschrig, and Bieger,[12,13] applies the formalism of optimized linear combination of atomic orbitals as introduced by Eschrig and Bergert for band-structure calculations.[14] In this approximation, the Kohn-Sham orbitals ψ_i of the system are expanded in terms of atom-centered localized basis functions ϕ_μ:

$$\psi_i(\mathbf{r}) = \sum_\nu C_{\nu i}\phi_\nu(\mathbf{r}-\mathbf{R}_k), \tag{1}$$

solving the Kohn-Sham equations in an effective one-particle potential $V_{\text{eff}}(\mathbf{r})$:

$$\hat{H}\psi_i(\mathbf{r}) = \varepsilon_i\psi_i(\mathbf{r}), \qquad \hat{H} = \hat{T} + V_{\text{eff}}(\mathbf{r}) . \tag{2}$$

As a result, the Kohn-Sham equations are transformed into a set of algebraic equations:

$$\sum_\nu C_{\nu i}(H_{\mu\nu} - \varepsilon_i S_{\mu\nu}) = 0, \quad \forall\mu, i , \tag{3}$$

where

$$H_{\mu\nu} = \langle\phi_\mu|\hat{H}|\phi_\nu\rangle, \qquad S_{\mu\nu} = \langle\phi_\mu|\phi_\nu\rangle . \tag{4}$$

As has already been shown by a variety of authors,[15–18] the total energy of the system can be approximated as a sum over the band-structure energy (sum of the eigenvalues of all occupied orbitals) and a short-range repulsive two-body potential:

$$\begin{aligned} E_{\text{tot}}(\{\mathbf{R}_k\}) &= E_{\text{BS}}(\{\mathbf{R}_k\}) + E_{\text{rep}}(\{|\mathbf{R}_k - \mathbf{R}_l|\}) \\ &= \sum_i n_i\varepsilon_i(\{\mathbf{R}_k\}) + \sum_k\sum_{<l} V_{\text{rep}}(|\mathbf{R}_l - \mathbf{R}_k|) , \end{aligned} \tag{5}$$

where n_i is the occupation number of orbital i.

In order to get the necessary matrix elements and the repulsive contributions V_{rep}, we perform the construction of our potential in three steps which are discussed in detail below: (a) Creation of (spin-unpolarized) pseudoatoms by solving a modified atomic Kohn-Sham equation; (b) calculation of all Hamiltonian and overlap matrix elements; and (c) fitting of the short-range repulsive potential V_{rep}.

Creation of the pseudoatoms

We write the pseudoatomic wave functions in terms of Slater-type orbitals and spherical harmonics:

$$\phi_\nu(\mathbf{r}) = \sum_{n,\alpha,l_\nu,m_\nu} a_{n\alpha} r^{l_\nu+n} e^{-\alpha r} \mathrm{Y}_{l_\nu m_\nu}\left(\frac{\mathbf{r}}{r}\right) . \tag{6}$$

As many tests have shown,[19] five different values of α and $n = 0, 1, 2, 3$ form a sufficiently accurate basis set for all elements up to the third row. Since the introduction of additional functions does not yield any significant changes, this basis can be considered converged.

Using ansatz (6), we perform a self-consistent solution of modified atomic Kohn-Sham equations:

$$[\hat{T} + V^{\text{psat}}(r)]\phi_\nu(\mathbf{r}) = \varepsilon_\nu^{\text{psat}}\phi_\nu(\mathbf{r}) , \tag{7}$$

$$\begin{aligned} V^{\text{psat}}(r) = V_{\text{nucleus}}(r) + V_{\text{Hartree}}[n(r)] \\ + V_{\text{xc}}^{\text{LDA}}[n(r)] + \left(\frac{r}{r_0}\right)^N . \end{aligned} \tag{8}$$

V_{xc} is expressed in terms of the local-density approximation as parametrized by Perdew and Zunger.[20] The additional term $(r/r_0)^N$ appearing in $V(r)$ in Eq. (8) was first introduced by Eschrig *et al.*[14,19] in order to improve band-structure calculations performed within LCAO. It forces the wave functions to avoid areas far away from the nucleus, thus resulting in an electron density that is compressed in comparison to the free atom. The parameter N has only a rather small influence on the results, we choose $N = 2$ for all types of atoms. The radius r_0 may be optimized to yield best results; however, we have found that $r_0 \approx 2r_{\text{cov}}$ is usually a good choice, where r_{cov} is the covalent radius of the element.

Calculation of matrix elements

We use the solutions ϕ_ν of Eq. (7) as the basis functions for the LCAO treatment of the system. Within a minimal basis description, only valence orbitals are considered. As an approximation, we write the one-electron potential of the many-atom structure as a sum of spherical atomic contributions:

$$V_{\text{eff}}(\mathbf{r}) = \sum_k V_0^k(|\mathbf{r} - \mathbf{R_k}|) , \tag{9}$$

where V_0 is the Kohn-Sham potential of a neutral pseudoatom, due to its *compressed* electron density, but not containing the additional term $(r/r_0)^N$ anymore. This ansatz differs from the one used in previous studies,[12,15,16] where the potentials of free neutral atoms were used to evaluate the matrix elements. Using the potentials of compressed pseudoatoms for the evaluation of the matrix elements has two advantages.

(i) Numerous self-consistent calculations on molecules and solids have shown that the electron densities in these structures can be roughly approximated as a superposition of *compressed* atomic densities. Thus, by using this information, we anticipate the results of a more sophisticated calculation up to a certain extent. In addition to that, as was already shown by Seifert *et al.*,[13] the densities due to superposed pseudoatomic potentials are even more realistic than a simple superposition of pseudoatomic densities.

(ii) The necessary integral approximations work better if one uses basis functions that decay more rapidly than those of the free atom. Furthermore, Eschrig and Bergert[14] has shown that the modified wave functions

form a better basis set in condensed matter applications. Similar ideas on confined orbitals have been discussed more recently by Jansen and Sankey[21] and Chetty *et al.*[22]

The overlap matrix consists only of two-center elements and can be calculated in a straightforward way. Consistent with Eq. (9), one can neglect several contributions to the Hamiltonian matrix elements $H_{\mu\nu}$,[12] yielding

$$H_{\mu\nu} = \begin{cases} \varepsilon_{\mu}^{\text{free atom}} & \text{if } \mu = \nu \\ \langle \phi_{\mu}^{A} | \hat{T} + V_0^A + V_0^B | \phi_{\nu}^{B} \rangle & \text{if } A \neq B \\ 0 & \text{otherwise.} \end{cases} \tag{10}$$

The indices A and B indicate the atom on which the wave functions and the potentials are centered. As can be seen easily, only two-center Hamiltonian matrix elements are treated. Approximation (10) may be seen as a LCAO variant of a cellular Wigner-Seitz method as applied, for instance, by Inglesfield.[23] As follows from Eq. (10), the eigenvalues of the free atom serve as diagonal elements of the Hamiltonian, thus guaranteeing the correct limit for isolated atoms.

Due to the fact that all matrix elements depend only on interatomic distances, we need to calculate them only once for each pair of atom types and store the values using a stepwidth of $0.1a_B$. For the two-center integral evaluation, the analytic formula of Eschrig[24] is applied. Matrix elements corresponding to a given interatomic distance can easily be obtained by interpolating between the stored values. Therefore, the creation of the Hamiltonian requires about the same time as in common TB models. The calculation time is mainly determined by the efficiency of the diagonalization routines. We are still using Householder and QL algorithms, but the implementation of recently developed linear scaling methods[25] is in progress.

Fitting of short-range repulsive part

The characterization of the Hamiltonian as described in the previous subsection allows one to calculate the band-structure energy E_{BS}. Thus, the short-range repulsive part $V_{\text{rep}}(R)$ can easily be determined as the difference of the total energy resulting from a self-consistent calculation and E_{BS} for different values of interatomic distances R:

$$V_{\text{rep}}(R) = E_{\text{LDA}}^{\text{sc}}(R) - E_{\text{BS}}(R) \, . \tag{11}$$

TABLE I. Coefficients and boundaries of the Chebyshev polynomial expansion for the Hamiltonian and overlap matrix elements versus interatomic distance $r \in$ (a,b) for C-C, C-H, and H-H interactions. Values for a and b are in bohrs, potential and Hamiltonian coefficients are in hartrees. A more detailed explanation is given in the text.

Matrix	c_1	c_2	c_3	c_4	c_5
(a,b)	c_6	c_7	c_8	c_9	c_{10}
$H_{ss\sigma}^{\text{CC}}$	−0.4663805	0.3528951	−0.1402985	0.0050519	0.0269723
(1.0,7.0)	−0.0158810	0.0036716	0.0010301	−0.0015546	0.0008601
$H_{sp\sigma}^{\text{CC}}$	0.3395418	−0.2250358	0.0298224	0.0653476	−0.0605786
(1.0,7.0)	0.0298962	−0.0099609	0.0020609	0.0001264	−0.0003381
$H_{pp\sigma}^{\text{CC}}$	0.2422701	−0.1315258	−0.0372696	0.0942352	−0.0673216
(1.0,7.0)	0.0316900	−0.0117293	0.0033519	−0.0004838	−0.0000906
$H_{pp\pi}^{\text{CC}}$	−0.3793837	0.3204470	−0.1956799	0.0883986	−0.0300733
(1.0,7.0)	0.0074465	−0.0008563	−0.0004453	0.0003842	−0.0001855
$S_{ss\sigma}^{\text{CC}}$	0.4728644	−0.3661623	0.1594782	−0.0204934	−0.0170732
(1.0,7.0)	0.0096695	−0.0007135	−0.0013826	0.0007849	−0.0002005
$S_{sp\sigma}^{\text{CC}}$	−0.3662838	0.2490285	−0.0431248	−0.0584391	0.0492775
(1.0,7.0)	−0.0150447	−0.0010758	0.0027734	−0.0011214	0.0002303
$S_{pp\sigma}^{\text{CC}}$	0.3715732	−0.3070867	0.1707304	−0.0581555	0.0061645
(1.0,7.0)	0.0051460	−0.0032776	0.0009119	−0.0001265	−0.0000227
$S_{pp\pi}^{\text{CC}}$	−0.1359608	0.0226235	0.1406440	−0.1573794	0.0753818
(1.0,7.0)	−0.0108677	−0.0075444	0.0051533	−0.0013747	0.0000751
$H_{ss\sigma}^{\text{CH}}$	0.3523274	−0.2827934	0.1408311	−0.0332928	−0.0073840
(1.0,7.0)	0.0102781	−0.0050642	0.0017970	−0.0005711	0.0001695
$H_{sp\sigma}^{\text{CH}}$	0.3597435	−0.2796815	0.1248796	−0.0207234	−0.0095584
(1.0,7.0)	0.0078841	−0.0035287	0.0016687	−0.0007754	0.0002626
$H_{ss\sigma}^{\text{HH}}$	−0.2794685	0.2233009	−0.1103361	0.0284041	−0.0004326
(1.0,6.0)	−0.0013758	−0.0001446	0.0002392	0.0000308	−0.0000531
$S_{ss\sigma}^{\text{CH}}$	−0.3852816	0.3085693	−0.1516239	0.0330417	0.0102731
(1.0,6.5)	−0.0107361	0.0034289	−0.0000651	−0.0003785	0.0001523
$S_{sp\sigma}^{\text{CH}}$	−0.4285567	0.3245500	−0.1234929	−0.0092742	0.0377529
(1.0,6.5)	−0.0200635	0.0042566	0.0006126	−0.0007052	0.0002143
$S_{ss\sigma}^{\text{HH}}$	0.3364029	−0.2824889	0.1645283	−0.0601065	0.0067570
(1.0,6.5)	0.0058363	−0.0035640	0.0008281	0.0000277	−0.0000713

We write $V_{\mathrm{rep}}(R)$ as a sum of polynomials:

$$V_{\mathrm{rep}}(R) = \begin{cases} \sum_{n=2}^{NP} d_n (R_c - R)^n & (R < R_c) \\ 0 & \text{otherwise.} \end{cases} \tag{12}$$

Ansatz (12) guarantees $V_{\mathrm{rep}}(R)$ to be zero for $R \geq R_c$ and a smooth behavior at the cutoff radius R_c. In many cases, this expression is sufficient enough to fit the points given by Eq. (11) using a maximum power of $NP = 5$. We expect the fit to be of similar or even better quality

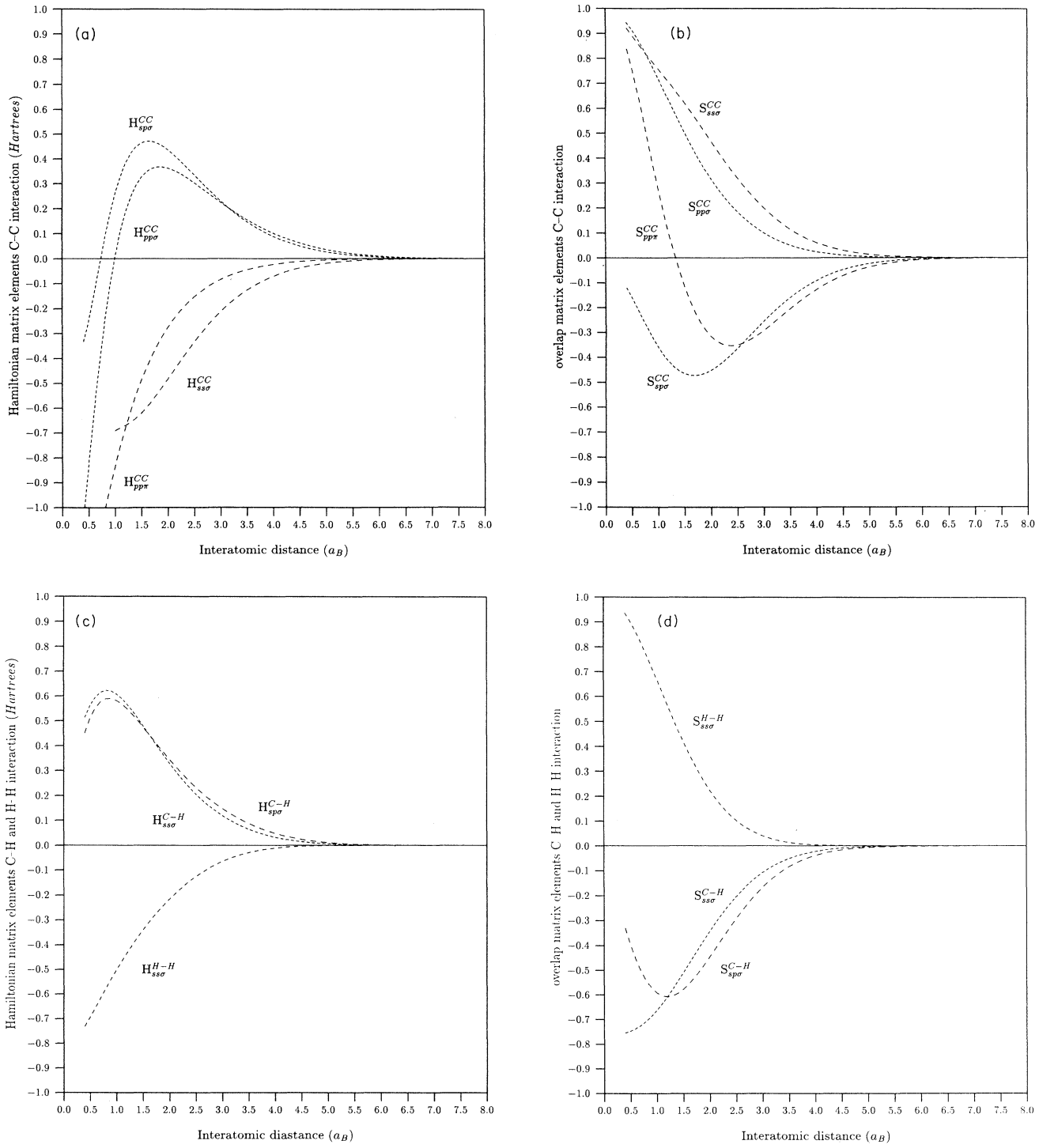

FIG. 1. Hamiltonian and overlap matrix elements versus interatomic separation: (a) $H^{\mathrm{C-C}}$, (b) $S^{\mathrm{C-C}}$, (c) $H^{\mathrm{C-H,H-H}}$, and (d) $S^{\mathrm{C-H,H-H}}$. Interval boundaries a and b are in bohrs, Hamiltonian matrix elements in hartrees.

if an exponential form of the repulsive potential is taken into consideration.

In most cases, diatomic molecules can be used to fit $V_{\rm rep}(r)$. However, these small systems sometimes tend to show level crossings causing sudden changes of orbital occupation numbers (as long as occupation numbers are restricted to integers) and thus discontinuities in the first derivatives of the energies. This behavior makes a reasonable fit in the vicinity of the level crossing almost impossible. Fortunately, one is not restricted to diatomic molecules. Every information available from self-consistent calculations can be included in the fit.

III. DETERMINATION OF THE PARAMETERS FOR C AND H

For carbon and hydrogen, we used 1.42 Å and 0.69 Å for the value of r_0 [see Eq. (8)]. This corresponds to 1.85 times the covalent radius of each element. The repulsive potential for the H-H and C-H interaction was fit to self-consistent LDA calculations of the diatomic molecules. Some problems arise when one tries to fit the C-C interaction only to the C_2 molecule. As self-consistent LDA calculations show, the σ_g and π_u state are almost degenerate and cross each other near the diamond equilibrium distance. There is no point in fitting $V_{\rm rep}(r)$ to the discontinuity in the first derivative of the total energy, due to this level crossing. Therefore, the bulk moduli of graphite and diamond have been used to model the curvature of $V_{\rm rep}(r)$ for $r > 1.4$ Å.

In Figs. 1(a)–1(d), we show the Hamiltonian and overlap matrix elements versus interatomic separation for carbon-carbon, carbon-hydrogen, and hydrogen-hydrogen inteactions. To derive analytical expressions for the Slater-Koster data, we expressed them in terms of Chebyshev polynomials yielding

$$V(r) = \sum_{m=1}^{10} c_m \, T_{m-1}(y) - \frac{c_1}{2}, \qquad y = \frac{r - \frac{b+a}{2}}{\frac{b-a}{2}} . \quad (13)$$

The resulting coefficients c_m and boundaries a and b of the expansion are given in Table I. The standard deviation achieved in all cases is less than 10^{-4}. Table II contains a corresponding representation of the short-range repulsive two-particle potentials. However, for all tests performed in the following sections, the exact values of the Slater-Koster tables have been used.

IV. TEST AND RESULTS

Small carbon clusters

The first group of systems we investigated with our method were carbon clusters. Table III shows the ground state geometries and zero-point energy corrected binding energies per atom for the small carbon clusters C_2 to C_{10}. We corrected our binding energies for the spin-polarization energy of the free carbon atom (1.13 eV), determined with a self-consistent LSDA method. The results are compared to *ab initio* calculations by Raghavachari and Binkley[7] and Almloef.[26] Though other TB calculations performed on such small systems often use an additional Hubbard-like term in the total-energy expression to describe charge transfer and correlation effects, we did not use this modification since we wanted to test the accuracy of our model without further changes.

The geometries of the small clusters are in good agreement with the *ab initio* results. Except for C_8, where our most stable ring has C_{8v} symmetry, the symmetry groups of our cyclic clusters are identical with those calculated on *ab initio* level. All bond angles are 5°–10° larger than the ones determined by the more complicated self-consistent method. The bond lengths of the cyclic structures are about 0.02 Å larger, whereas those of the linear forms alternate stronger than the ones determined by the self-consistent calculation. Because the largest discrepancies appear at the ends of the chains, it is likely that they are mainly caused by strong correlation effects and charge transfers that differ slightly from the self-consistent calculations. However, the errors in the bond lengths are in no case larger than 5%, typically 2–3 %. Our calculations show that from C_2 to C_9 the linear forms are the most stable ones, though the even-numbered cyclic structures are almost comparable in energy. In contrast to that, the calculations of Raghavachari and Binkley[7] found cyclic C_4, C_6, and C_8 to be more stable than the linear chains. We want to note, however, that the energy difference for all these structures is rather small and that the HF energies in

TABLE II. Coefficients and boundaries of the Chebyshev polynomial expansion for the short-range repulsive potential versus interatomic distance $r \in$ (a,b) for C-C, C-H, and H-H interactions. Values for a and b are in bohrs, potential coefficients are in hartrees. A more detailed explanation is given in the text.

$V_{\rm rep}$	c_1	c_2	c_3	c_4	c_5
(a,b)	c_6	c_7	c_8	c_9	c_{10}
$V_{\rm rep}^{\rm CC}$	2.2681036	-1.9157174	1.1677745	-0.5171036	0.1529242
(1.0,4.10)	-0.0219294	-0.0000002	-0.0000001	-0.0000005	0.0000009
$V_{\rm rep}^{\rm CH}$	0.4679363	-0.3651743	0.1906972	-0.0841604	0.0285450
(1.0,3.70)	-0.0038757	0.0000000	0.0000000	-0.0000001	0.0000002
$V_{\rm rep}^{\rm HH}$	0.1432403	-0.0985304	0.0338895	-0.0116796	0.0062808
(1.0,3.11)	-0.0028892	0.0010845	0.0006418	-0.0001857	-0.0002322

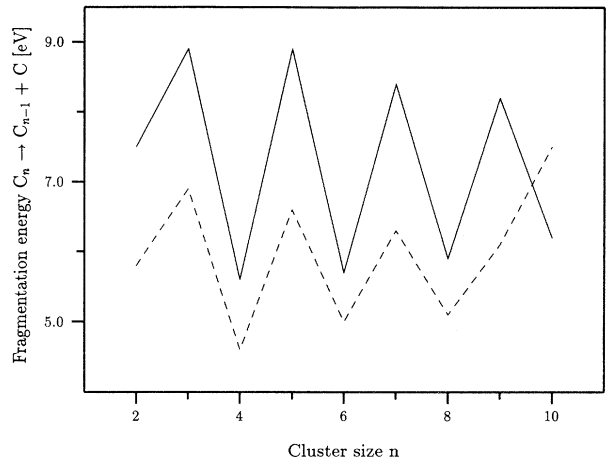

FIG. 2. Energies of the fragmentation reaction $C_n \rightarrow C_{n-1}$ + C calculated within LDA-TB (solid line) and *ab initio* CCD+STD(CCD) (dashed line) versus cluster size.

the *ab initio* calculations (which were used to optimize geometries) favor the linear forms just like our method does.

A very interesting test is to calculate the energy of the reaction $C_n \rightarrow C_{n-1}$ + C for each cluster and plot it as a function of n as was done in Fig. 2. The shape of the DF-TB curve is very similar to the one of the self-consistent calculation. There are, of course, some discrepancies. All energies are too large by a little more than 1 eV. We expected this behavior since LDA typically overestimates binding energies. We also do not find the change in the even-odd behavior of the fragmentation energies observed by Raghavachari *et al.* for C_{10}. Furthermore, the difference in the fragmentation energies between even and odd numbered clusters is even larger than in the *ab initio* calculation. This problem could probably be solved by introducing an additional term in the Hamiltonian accounting explicitly for correlation and charge transfer effects.

C_{60}

The C_{60} cluster is a very interesting object because it can be considered as a system between a typical molecular and a typical solid-state structure. For that reason, we calculated the ground state geometry, total energy, and phonon frequencies within our model. The results are listed in Table IV.

We find the two different bond lengths to be 1.397 Å and 1.449 Å, which is in very good agreement with the experimental 1.402 Å and 1.462 Å, as well as with the 1.398 Å and 1.450 Å determined by self-consistent LDA calculations.[27] The binding energy of each atom in the cluster is 8.85 eV, with respect to the free spin-unpolarized atom. This value has to be seen in relation to the 9.22 eV calculated for the diamond structure—see be-

TABLE III. Bond lengths, angles, and binding energies per atom for the clusters C_2 through C_{10}. For the linear molecules, bond lengths are sorted beginning at the end of the chains. Binding energies are with respect to the free, spin-polarized carbon atom (see text). Reference values for CCD+STD(CCD) were taken from Ref. 7 and for CASSCF from Ref. 26.

Cluster	Method	Symm.	Bond lengths (Å)	Angle	E_{bind}^{at} (eV)
C_2	DF-TB	$D_{\infty h}$	1.244	180.0	3.7
	CCD	$D_{\infty h}$	1.245	180.0	2.9
C_3	DF-TB	$D_{\infty h}$	1.288	180.0	5.5
	CCD	$D_{\infty h}$	1.278	180.0	4.2
C_4	DF-TB	$D_{\infty h}$	1.288 1.321	180.0	5.5
	CASSCF[a]	$D_{\infty h}$	1.306 1.287	180.0	
	DF-TB	D_{2h}	1.443	70.7	5.1
	CCD	D_{2h}	1.425	61.5	4.3
	CASSCF[a]	D_{2h}	1.432	64.5	
C_5	DF-TB	$D_{\infty h}$	1.257 1.315	180.0	6.2
	CCD	$D_{\infty h}$	1.271 1.275	180.0	4.8
C_6	DF-TB	$D_{\infty h}$	1.265 1.324 1.287	180.0	6.1
	DF-TB	D_{3h}	1.346	100.1	5.8
	CCD	D_{3h}	1.316	90.4	4.8
C_7	DF-TB	$D_{\infty h}$	1.245 1.337 1.280	180.0	6.4
	CCD	$D_{\infty h}$	1.270 1.280 1.264	180.0	5.0
C_8	DF-TB	$D_{\infty h}$	1.253 1.335 1.279 1.308	180.0	6.4
	DF-TB	C_{8v}	1.348	120.3	6.2
	CCD	D_{4h}	1.240 1.380	107.1	5.0
C_9	DF-TB	$D_{\infty h}$	1.240 1.350 1.263 1.302	180.0	6.6
	CCD	$D_{\infty h}$	1.269 1.283 1.261 1.269	180.0	5.2
C_{10}	DF-TB	$D_{\infty h}$	1.246 1.345 1.269 1.311 1.284	180.0	6.5
	DF-TB	D_{5h}	1.311	125.3	6.5
	CCD	D_{5h}	1.290	119.4	5.4

low. Therefore, our model yields an energy difference of 0.37 eV between C_{60} and the diamond structure, which is in good agreement with more sophisticated calculations[28] estimating this difference to be 0.3–0.4 eV.

The phonon frequencies of C_{60} were determined using the relaxed geometry and applying the same scheme as Quong *et al.*[27] Since only a few of the modes are experimentally observable, we compare our results with two LDA calculations performed independently by different authors[27,29] and define the error of the frequencies with respect to the average of the two LDA methods. As can be seen from Table IV, the general properties of the phonon spectrum are well described with a maximal error of 17% (for the second T_{1u} mode) and an average error of 10%. Especially most of the low energy modes are very close to those of the LDA calculations. The high energy modes, however, are between 10% and 15% too large. Analyzing the eigenvectors of the vibrations yields the result that the largest discrepancies occur for phonons with a high percentage of C-C stretching. For that reason, we believe that a more sophisticated fit of the short-range repulsive potential could make this systematic errors even smaller.

Hydrocarbons

Carbon shows many different types of bonding. All of them can be found in the huge class of molecules known as hydrocarbons. For that reason, it is important to know how a method performs on these systems. In addition, hydrocarbons are well understood and one can refer to an abundant number of experimental and theoretical data. For all the properties tested here, accurate self-consistent calculations are available.[28,30–32] Table V shows the ground state geometries of the radicals CH, CH_2, and CH_3 and the molecules H_2, CH_4, C_2H_2, C_2H_4, C_2H_6, C_6H_6, cyclopropene C_3H_4, cyclopropane C_3H_6 and *n*-butane C_4H_{10}. We want to note here that according to experiments all the radicals are spin polarized, therefore a direct comparison is difficult for these structures. This is especially true for CH_2, where the absence of spin in our model leads to a more stable singlet state. For that reason, we compare our geometries for this radical with spin-unpolarized calculations and the experimentally observable singlet state.

As in SCF-LDA calculations, the C-C and H-H single bond lengths are about 0.02 Å too short in comparison to experimental data. The double bond in C_2H_4 is about 0.01 Å too short, while the triple bond in C_2H_2 has almost the same length as known from experiments. Structures with very small C-C-C bond angles, such as cyclopropane and cyclopropene, are also well described. C-H bonds are systematically overestimated by about 0.03 Å, a little bit more than the overestimation in SCF-LDA calculations. Bond angles agree within 2° or even better; exceptions are the radicals where the H-C-H angles are

TABLE IV. Harmonic vibrational frequencies (cm^{-1}) for the fullerene cluster C_{60} in comparison to SCF-LDA calculations performed by Quong (Ref. 27) and Wang (Ref. 29). Total energies and bond lengths are given in the text.

Rep.	DF-TB	Quong	Wang	Err. (%)	Rep.	DF-TB	Quong	Wang	Err. (%)
A_g	552	478	483	+14.9	A_u	1017	850	947	+13.2
	1683	1499	1529	+11.2					
					T_{1u}	512	547	533	−4.2
T_{1g}	589	580	566	+2.8		656	570	548	+17.3
	886	788	825	+9.9		1326	1176	1214	+11.0
	1442	1252	1292	+13.4		1642	1461	1485	+11.5
T_{2g}	563	547	550	+2.6	T_{2u}	354	342	344	+3.2
	736	610	771	+6.7		704	738	717	−3.2
	863	770	795	+10.3		1094	962	987	+12.3
	1540	1316	1360	+15.1		1352	1185	1227	+12.1
						1754	1539	1558	+13.3
G_g	500	486	484	+3.1					
	605	571	564	+6.6	G_u	360	356	356	+1.1
	743	759	763	−2.4		745	683	752	+3.8
	1223	1087	1117	+11.0		819	742	784	+7.3
	1461	1296	1326	+11.4		1076	957	977	+11.3
	1728	1505	1528	+13.9		1494	1298	1339	+13.3
						1645	1440	1467	+13.2
H_g	271	258	263	+4.0					
	434	439	432	−0.3	H_u	417	404	396	+4.2
	714	727	713	−0.8		554	539	534	+3.3
	868	767	778	+12.4		698	657	663	+5.8
	1247	1093	1111	+13.2		751	737	742	+1.5
	1435	1244	1282	+13.6		1377	1205	1230	+13.1
	1635	1443	1469	+12.3		1521	1360	1358	+11.9
	1810	1576	1598	+14.1		1803	1565	1588	+14.4

TABLE V. Geometric properties obtained for selected radicals and molecules. All bond lengths are in Å. The SCF and experimental values have been taken from Ref. 31 (H_2 through ethane) and Ref. 30 (cyclopropene through benzene). GGA values refer to calculations using generalized gradient approximations for the exchange-correlation functional as described in Refs. 31 and 30.

Molecule	Variable	DF-TB	LSD	GGA	Exp.
H_2	HH	0.765	0.765	0.748	0.741
CH	CH	1.138	1.152	1.108	1.120
CH_2	CH	1.134	1.135	1.117	1.111
(Singlet)	HCH	98.6	99.1	99.1	102.4
CH_3	CH	1.114	1.093	1.090	1.079
	HCH	116.8	120.0	120.0	120.0
CH_4	CH	1.116	1.101	1.100	1.086
C_2H_2	CC	1.206	1.212	1.215	1.203
(acetylene)	CH	1.099	1.078	1.073	1.061
C_2H_4	CC	1.321	1.331	1.341	1.339
(ethene)	CH	1.113	1.098	1.095	1.085
	CCH	116.3	116.4	116.2	117.8
C_2H_6	CC	1.503	1.513	1.541	1.526
(ethane)	CH	1.119	1.105	1.104	1.088
	HCH	108.0	107.2	107.5	107.4
C_3H_4	C_1C_2	1.318	1.305		1.296
(cyclopropene)	C_2C_3	1.509	1.510		1.509
	C_1H	1.109	1.091		1.072
	HC_1C_2	148.4	149.5		149.9
C_3H_6	CC	1.503	1.504		1.510
(cyclopropane)	CH	1.114	1.095		1.089
C_4H_{10}	C_1C_2	1.511	1.517		1.533
(*n*-butane)	C_2C_3	1.520	1.532		1.533
C_6H_6	CC	1.389	1.396		1.399
(benzene)	CH	1.114	1.095		1.089

clearly underestimated by about 4°.

Table VI shows atomization energies (including zero-point corrections) and reaction energies for some typical hydrocarbon reactions. The atomization energies are with respect to free, *spin-polarized* atoms; that means the spin polarization energies of free carbon and hydrogen atoms (1.13 eV and 0.90 eV, respectively, calculated within LSDA) have been subtracted from the actual atomization energies determined by the DF-TB method. The atomization energies as taken from Ref. 28 are already corrected for zero-point vibrations. For the selected reaction energies presented here, accurate calculations and experimental values are available from Refs. 30 and 31.

It is interesting that the typical LDA overbinding effects cannot be found in the expected magnitude when applying the DF-TB formalism. The root mean square error per bond is only 3.5 kcal/mol for the molecules tested here. In particular, if one assumes an overbinding of 11 kcal/mol for each C-C single, double, and triple bond and no overbinding of C-H bonds, the absolute error of the atomization energies does not exceed 5 kcal/mol for all tested molecules. On the other hand, the reaction energies calculated self-consistently show a better error cancellation than DF-TB. Furthermore, the energies of the isodesmic reactions with cyclopropane and cyclopropene are clearly too large.

To test the dynamical properties of our potential, we have also determined the phonon frequencies for a number of radicals and molecules using the same method as for C_{60}. The results are displayed in Tables VII and VIII. It has already been outlined by some authors[30,31] that the frequencies determined this way have to be compared

TABLE VI. Atomization and reaction energies for some typical reactions of organic chemistry. Atomization energies are with respect to the free spin-polarized atoms (see text). Calculated energies are not corrected for zero-point vibrations, but experimental values are extrapolated to zero and corrected for zero-point vibrations. All reference energies were taken from Ref. 28 (atomization) and Ref. 30 (reactions).

	Atomization energies (kcal/mol)				
Molecule	DF-TB	HF	LSD	GGA	Exp.
H_2	113	84	113	105	109
CH_4	425	332	463	422	424
C_2H_2	422	300	461	417	408
C_2H_4	577	431	634	574	568
C_2H_6	735	557	795	720	719
C_6H_6	1438	1041	1577	1413	1375
Rms err/bond	3.5	27.4	12.9	2.5	
	Reaction energies (kcal/mol)				
Reaction	DF-TB	HF	LSD	GGA	Exp.
$C_2H_6 + H_2 \rightarrow 2\ CH_4$	2	21	18	19	19
$C_2H_4 + 2\ H_2 \rightarrow 2\ CH_4$	47	64	67	60	57
$C_2H_2 + 3\ H_2 \rightarrow 2\ CH_4$	89	118	131	114	89
Rms error	14.3	8.6	16.1	5.5	
$C_2H_4 + 2\ CH_4 \rightarrow 2\ C_2H_6$	43	22	32	22	20
$C_2H_2 + 4\ CH_4 \rightarrow 3\ C_2H_6$	84	54	77	58	49
$C_3H_4 + 3\ CH_4 \rightarrow 2\ C_2H_6 + C_2H_4$	87	50	50	44	45
$C_3H_6 + 3\ CH_4 \rightarrow 3\ C_2H_6$	63	26	26	23	25
Rms error	35.2	3.7	15.4	4.7	

TABLE VII. Calculated phonon modes (cm^{-1}) for selected hydrocarbons. Experimental frequencies are harmonic unless marked with n.h. in the field used for the relative errors. Relative errors are defined with respect to harmonic experimental frequencies. Reference values were taken from Ref. 31.

Mol.	Rep.	DF-TB	LSD	Exp.	Err. (%)	Rep.	DF-TB	LSD	Exp.	Err. (%)
H_2	Σ_g	4345	4207	4401	−1.3					
CH	Σ	2852	2682	2862	−0.3					
CH_2	A_1	1534	1392	1353	n.h.	B_2	2932	2844	2865	n.h.
		2892	2757	2806	n.h.					
CH_3	A_1	1534	1392	1353	n.h.	E	1374	1356	1396	n.h.
	A_2	651	488	606	n.h.					
CH_4	A_1	3006	2988	3137	−4.1	T_2	1378	1293	1357	+1.5
	E	1559	1526	1567	−0.5		3155	3121	3158	−0.1
C_2H_2	Σ_g	2297	2041	2011	+14.3	Π_g	544	475	624	−12.8
		3453	3452	3497	−1.3	Π_u	709	730	747	−5.1
	Σ_u	3292	3349	3415	−3.6					
C_2H_4	A_g	1363	1345	1370	−0.5	B_{2g}	869	910	959	−9.4
		1928	1685	1655	+16.5	B_{2u}	769	800	843	−8.8
		3121	3089	3153	−1.0		3213	3175	3234	−0.6
	A_u	1066	1036	1044	+2.1	B_{3g}	1227	1187	1245	−1.4
	B_{1u}	1431	1417	1473	−2.8		3202	3151	3232	−0.9
		3107	3073	3147	−1.3	B_{3u}	896	926	969	−7.5
C_2H_6	A_{1g}	1116	1038	1016	+9.8	E_g	1247	1178	1246	+0.0
		1489	1390	1449	+2.8		1509	1463	1552	−2.8
		3038	2978	3043	−0.2		3129	3045	3175	−1.5
	A_{1u}	188	317	303	−37.9	E_u	811	800	822	−1.3
	A_{2u}	1447	1360	1438	+0.6		1522	1466	1526	−0.3
		3049	2982	3061	−0.4		3140	3069	3140	+0.0

with *harmonic* experimental frequencies. When possible, this is done in this paper.

It is worth noting that for all frequencies around 3000 cm^{-1}, which correspond mainly to C-H stretching, the relative errors are typically only 1% and 4% at most. This is a very encouraging result since only the CH molecule has been used in the fit of the short-range part of the potential. As already found in C_{60}, the C-C stretching modes are too high by typically 10–15 %. For all other modes, the error is about 5% or even smaller. Exceptions are the π_g mode in C_2H_2, where SCF-LDA performs even worse, and the low-lying B_{2g}, B_{2u}, and B_{3u} modes in ethene are all too low compared to the experiment. Furthermore, the mode corresponding to the rotation of ethane around the C-C axis is far too low, indicating that the rotational barrier can be described only qualitatively. The average error is a little less than 10% and mainly determined by the C-C stretching modes.

Solids

There has been much progress in the application of TB models to solid-state modifications of carbon during the past few years.[9,33] For comparison, the results of accurate self-consistent methods are available for diamond and graphite[34,35] and high pressure modifications.[36] We performed calculations for the total energy as a function of nearest neighbor distance for the experimentally observed diamond and graphite lattices as well as for the

TABLE VIII. Calculated phonon modes (cm^{-1}) for the benzene molecule. All reference values were taken from Ref. 32, experimental frequencies are harmonic.

Mol.	Rep.	DF-TB	GGA	Exp.	Err. (%)	Rep.	DF-TB	GGA	Exp.	Err. (%)
C_6H_6	A_{1g}	1192	1015	1008	+18.3	E_{1g}	834	848	847	−1.5
		3207	3195	3191	+0.5	E_{1u}	1146	1057	1058	+8.3
	A_{2g}	1421	1360	1367	+4.0		1655	1500	1494	+10.8
	A_{2u}	646	649	686	−5.8		3208	3191	3181	+0.8
	B_{1u}	1047	1040	1024	+2.2	E_{2g}	624	617	613	+1.8
		3197	3174	3174	+0.7		1207	1178	1178	+2.5
	B_{2g}	691	723	718	−3.8		1873	1613	1607	+16.6
		963	998	990	−2.7		3203	3170	3174	+0.9
	B_{2u}	1176	1168	1167	+0.8	E_{2u}	399	401	407	−2.0
		1515	1435	1386	+9.3		950	971	967	−1.8

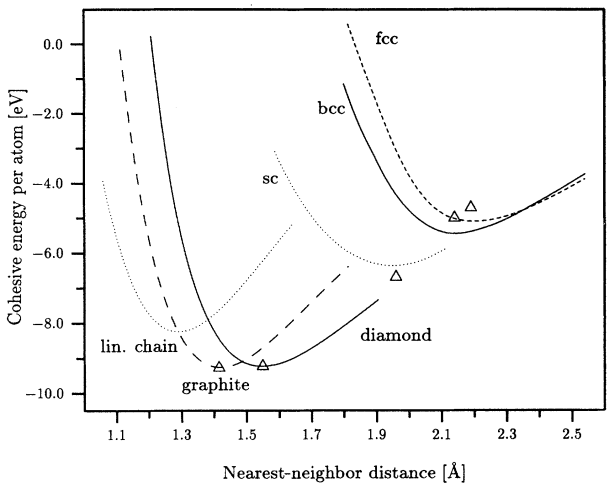

FIG. 3. Cohesive energies per carbon atom for different lattice types versus nearest neighbor distance. The inserted triangles give the reference energies of the SCF calculations (Refs. 34–36) with respect to the diamond cohesive energy.

linear chain, simple cubic (sc), fcc, and bcc structures. The results are displayed in Fig. 3. As one can see, the diamond and graphite phase are almost isoenergetic having a total energy of 9.22 eV and 9.24 eV, respectively. The above values are given with respect to the free spin-unpolarized atom. If one subtracts the spin-polarization energy of the free atom from these values, one yields about 8.1 eV per atom and thus a smaller overbinding of the C atoms compared to self-consistent LDA calculations. This behavior is consistent with those of the atomization energies as described in the previous section. The equilibrium distances and energetic positions of the high pressure modifications and the linear chain are also fairly well described, though the curvature is slightly too high for the sc, bcc, and fcc structures in comparison to the SCF-LDA calculation.[36] The determination of vibrational properties for diamond and graphite including some surfaces is in progress and will be examined in a separate work.

V. SUMMARY

We have presented a scheme for the determination of Hamiltonian and overlap matrix elements on the basis of density-functional theory in the framework of a method similar to widely used nonorthogonal semiempirical tight-binding schemes. By only incorporating two-center Hamiltonian integrals in the calculations, the usual short-range repulsive interaction appearing in TB models is fitted to self-consistent data derived in LDA. Despite its extreme simplicity, above all the complete neglection of three-center integrals, the potential is transferable without additional changes to the total-energy expression and gives reliable results for geometries, cohesive energies, and vibrational modes for the clusters, fullerenes, hydrocarbons, and solids. Except for a few systematic errors, phonon frequencies can be found within 10% of the experimental values. Atomization energies of hydrocarbons show less overbinding than in self-consistent LDA calculations, whereas the energies of typical reactions appearing in organic chemistry display the right behavior, but show also larger errors than those obtained by full *ab initio* methods.

ACKNOWLEDGMENTS

We gratefully acknowledge support from the Deutsche Forschungsgemeinschaft. We want to thank M. R. Pederson and B. N. Davidson for many interesting and stimulating discussions.

* Present address: Complex Systems Theory Branch, Naval Research Laboratory, Washington, D.C. 20375.

[1] J. Tersoff, Phys. Rev. Lett. **56**, 632 (1986); Phys. Rev. B **37**, 6991 (1988); Phys. Rev. Lett. **61**, 2879 (1988).
[2] D. W. Brenner, Phys. Rev. B **42**, 9458 (1990).
[3] R. Car and M. Parinello, Phys. Rev. Lett. **55**, 2471 (1985).
[4] M. R. Pederson and K. A. Jackson, Phys. Rev. B **41**, 7453 (1990).
[5] O. F. Sankey and D. J. Niklewski, Phys. Rev. B **40**, 3979 (1989).
[6] D. A. Drabold, P. A. Fedders, and P. Stumm, Phys. Rev. B **49**, 16 415 (1994).
[7] K. Raghavachari and J. S. Binkley, J. Chem. Phys. **87**, 2191 (1987).
[8] K. Laasonen and R. M. Nieminen, J. Phys. Condens. Matter **2**, 1509 (1990).
[9] C. H. Xu, C. Z. Wang, C. T. Chan, and K. M. Ho, J. Phys. Condens. Matter **4**, 6047 (1992).
[10] M. Menon and K. R. Subbaswamy, Phys. Rev. B **47**, 12 754 (1993).
[11] L. M. Canel, A. E. Carlsson, and P. A. Fedders, Phys. Rev. B **48**, 10 739 (1993).
[12] G. Seifert and H. Eschrig, Phys. Status Solidi B **127**, 573 (1985).
[13] G. Seifert, H. Eschrig, and W. Bieger, Z. Phys. Chem. (Leipzig) **267**, 529 (1986).
[14] H. Eschrig and I. Bergert, Phys. Status Solidi B **90**, 621 (1978).
[15] G. Seifert and R. O. Jones, Z. Phys. D **20**, 77 (1991).
[16] P. Blaudeck, T. Frauenheim, D. Porezag, G. Seifert, and E. Fromm, J. Phys. Condens. Matter **4**, 6389 (1992).
[17] W. M. C. Foulkes and R. Haydock, Phys. Rev. B **39**, 12 521 (1989).
[18] D. Tomanek and M. A. Schluter, Phys. Rev. B **36**, 1208 (1987).
[19] H. Eschrig, *Optimized LCAO Method and the Electronic Structure of Extended Systems* (Akademie-Verlag, Berlin, 1988).

[20] J. P. Perdew and A. Zunger, Phys. Rev. B **23**, 5048 (1981).
[21] R. Jansen and O. F. Sankey, Phys. Rev. B **36**, 6520 (1987).
[22] N. Chetty, K. Stokbro, K. W. Jakobsen, and J. K. Norskov, Phys. Rev. B **46**, 3798 (1992).
[23] J. E. Inglesfield, Mol. Phys. **37**, 873 (1979).
[24] H. Eschrig, Phys. Status Solidi B **96**, 329 (1979).
[25] P. Ordejon, D. A. Drabold, R. M. Martin, and M. P. Grumbach, Phys. Rev. B **48**, 14 646 (1993); **51**, 1456 (1995).
[26] V. Parasuk and J. Almloef, J. Chem. Phys. **94**, 8172 (1991).
[27] A. A. Quong, M. R. Pederson, and J. L. Feldman, Solid State Commun. **87**, 535 (1993).
[28] J. P. Perdew, J. A. Chevary, S. H. Vosko, K. A. Jackson, M. R. Pederson, D. J. Singh, and C. Fiolhais, Phys. Rev. B **46**, 6671 (1992).
[29] X. Q. Wang, C. Z. Wang, and K. M. Ho, Phys. Rev. B **48**, 1884 (1993).
[30] J. Andzelm and E. Wimmer, J. Chem. Phys. **96**, 1280 (1992).
[31] B. G. Johnson, P. M. W. Gill, and J. A. Pople, J. Chem. Phys. **98**, 5612 (1993).
[32] N. C. Handy, P. E. Maslen, R. D. Amos, J. S. Andrews, C. W. Murray, and G. J. Laming, Chem. Phys. Lett. **197**, 506 (1992).
[33] B. N. Davidson and W. E. Pickett, Phys. Rev. B **49**, 11 253 (1994).
[34] M. T. Yin and M. L. Cohen, Phys. Rev. B **24**, 6121 (1981).
[35] M. T. Yin and M. L. Cohen, Phys. Rev. B **29**, 6996 (1984).
[36] S. Fahy and S. G. Louie, Phys. Rev. B **36**, 3373 (1987).